

Nucleation of crystals at the bcc-hcp transition line in solid ^4He

M. Maekawa, Y. Okumura, and Y. Okuda

Department of Condensed Matter Physics, Tokyo Institute of Technology, 2-12-1, Oh-okayama, Meguro-ku, Tokyo 152-8551, Japan

(Received 12 April 2001; revised manuscript received 16 November 2001; published 4 April 2002)

The nucleation phenomenon in the structural transition between the bcc and hcp phase of solid ^4He on the melting line was investigated. At the lower transition point T_{c1} (1.457 K), the transition was triggered by a single new phase seed nucleated on the wall in contact with the superfluid and the seed grew up into the superfluid region. The nucleation of the new phase has nothing to do with the original solid. The situation is almost the same for the two cases of bcc to hcp (cooling) and hcp to bcc (warming) transitions, whereas at the higher transition temperature T_{c2} (1.778 K), where the crystal coexisted with normal liquid, the new phase seeds were nucleated at many sites inside the original crystal and the crystal was cracked into many grains. This is strongly reminiscent of martensitic transition. The supercooling and superheating phenomena observed in those transitions were analyzed based on the standard homogeneous nucleation theory, though it is clear that those transitions are nucleated heterogeneously. The temperature width of supercooling is larger than that of superheating at T_{c1} , whereas it is larger for superheating at T_{c2} . That is, supercooling (and superheating) is more likely in the transition from bcc to hcp regardless of warming or cooling. The transition event rate, $\Sigma = (N_0 - N)/N_0$, is well reproduced by the formula $\Sigma = (N_0 - N)/N_0 = 1 - \exp[-(\delta T/c)\Gamma_0 \exp(-\Delta E/kT)]$. The transition barrier ΔE is estimated by the fitting.

DOI: 10.1103/PhysRevB.65.144525

PACS number(s): 67.80.-s, 67.40.-w, 81.10.Aj, 64.60.Qb

I. INTRODUCTION

^4He crystal in equilibrium with superfluid at low temperature is an ideal system for the study of any crystal-related physics. In addition to the fact that ^4He in the low-temperature region is ultimately pure in itself, crystal growth of solid ^4He is very unique.¹ As solid ^4He is grown from superfluid and the latent heat is very small, its growth coefficient is enormously large, so the thermal equilibrium is attained in a very small time scale. The true equilibrium crystal shape is observable for a macroscopic crystal size.

Such ^4He crystal can also be an ideal system to investigate the nucleation physics at low temperature, and there have already been several experiments performed in this context.² This paper is focused on the nucleation in the solid-solid transition of ^4He , which has not yet been investigated.

Solid ^4He has two structural phases on the melting pressure: bcc and hcp. The lower transition point $T_{c1} = 1.457$ K co-exists with superfluid, whereas the higher transition point $T_{c2} = 1.778$ K with normal liquid. Thus, comparing the findings based on these two transition points, it is possible to determine the essential role of superfluid on the nucleation in the structural phase transition.

The nucleation at these transition temperatures is assumed to be triggered by the thermal activation. The fluctuation has to go over the free energy barrier as Eq. (1),

$$F = 4\pi\sigma r^2 - \frac{4}{3}\pi r^3\Delta G, \quad (1)$$

where σ is the surface tension between the nucleated seed and the host crystal, and ΔG is the gain of the bulk free energy.

The equation of the state of solid ^4He is still far from being fully understood except for the ground-state energy, in spite of its simple character. The phase diagram, which has a very small bcc region between 1.457 and 1.778 K, has not yet been reproduced from the first-principle calculation. One

reason is that the ground-state energy difference between hcp and bcc is so small and the equilibrium state is very sensitive to a tiny long-range interaction.^{5,6} On the other hand, the surface tension difference between hcp solid and bcc solid against superfluid is estimated to be on the order of 0.1 erg/cm^2 ,⁷ which is quite large with respect to the bulk free-energy difference. This means that large supercooling or superheating could occur during the transition. A simple calculation gives unbelievably small transition probability even at 1 K, based on the standard homogeneous nucleation model. But we actually observed the transition, thus there must be something external which triggers it. Very similar situations in other systems are discussed at ultralow temperature.^{8,9}

It is interesting to see how supercooling and superheating are observed in these structural transitions of solid ^4He . And it should also be very interesting to see how the crystal shape changes where superfluid co-exists. This can be studied by direct optical observation of the ^4He crystal.

Structural transition often exhibits the martensitic transition. For example, in some alkali metals, such as Na, K, and Li, the martensitic transition has been studied intensively.¹⁰⁻¹² Solid ^4He is also an ideal system with which to investigate the martensitic transition, and the nucleation study of ^4He will provide important insight into this transition.

II. EXPERIMENTS

The experimental setup was almost the same as that reported previously.¹³ The cell body was machined out of an oxygen-free high-conductivity copper block as shown in Fig. 1. It had two optical windows in the horizontal direction. These windows were made of a 20-mm-diameter \times 7-mm-thick sapphire plate, which was glued into the stainless frame with kovar alloy. The stainless frame was attached to the cell body by In wire seal. The kovar seal was perfect up to 30

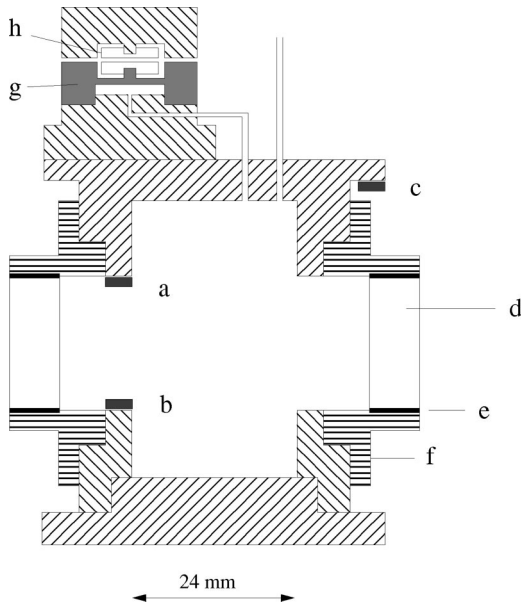


FIG. 1. A schematic picture of the sample cell. a and b are germanium resistance thermometers, c is the ruthenium oxide thermometer, d is the sapphire window, e is the kovar seal, f is the stainless frame of the window, g is the BeCu strain sensor, and h is the capacitance plate.

bars in the low temperature for many thermal cycles. This type of optical window can be the most reliable one for the present purpose.¹⁴ The sample cell was attached to the charcoal-operated ³He cryostat.

The thermometers were two germanium resistors (a and b in Fig. 1) and one ruthenium oxide resistor (c in Fig. 1). One was placed in the upper part of the inside of the cell and the other in the lower part, so that they could monitor liquid and solid temperature directly. The third one was attached to the outside wall of the sample cell, and was used to control the temperature of the system. The temperature was controlled by changing the heat current through the heater on the ³He pot. Calibration of the thermometers was done by comparing the measured melting curve and the lambda line with those in the literature.¹⁶ The experiment was performed keeping the crystal in the lower half of the sample cell. The transition point was swept slowly along the melting curve. The crystal shape was monitored through a charge-coupled device (CCD) camera together with the pressure and temperature measurement.

The pressure sensor was made of Be-Cu alloy following the design of the Straty-Adams-type gauge.¹⁵ The pressure gauge was attached to the top of the cell to monitor the pressure of the liquid. The pressure was measured by an autocapacitance bridge¹⁷ with the excitation voltage of 1 V. Capacitance-pressure calibration was done at 1.8 K using the diaphragm-type pressure gauge at room temperature,¹⁸ and the pressure was controlled by regulating the pressure of a buffer tank at room temperature.

III. RESULTS AND DISCUSSION

A. Crystal shape just at the transition

We first discuss the result at T_{c1} . Figures 2 and 3 show

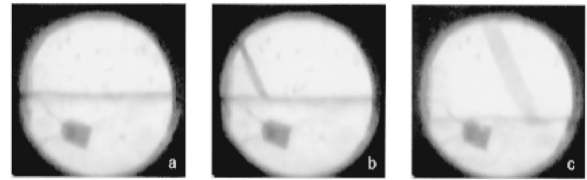


FIG. 2. Crystal shapes at the transition of T_{c1} in the cooling process. A new crystal is coming from the left (inclined line). (a) is the picture just before the hcp crystal comes into view. In (c) the inclined line has become thicker. This is due to the misalignment between the CCD camera and the plane. The period from (a) to (c) is about 500 msec. The horizontal line indicates the original bcc crystal.

pictures of the new phase crystal growing just at T_{c1} . Figure 2 is the transition from bcc to hcp (cooling) and Fig. 3 is that from hcp to bcc (warming). Figures 2 and 3 show the time sequence of the crystal growth of the nucleated seed from left to right. The time interval from left to right was about 0.5 sec for each figure.

In Fig. 2, the crystal with a flat inclined surface is the new hcp crystal coming out from the left-hand side. The horizontal line is the interface between bcc (original) crystal and superfluid. In Fig. 3, a rounded crystal is bcc crystal also coming out from the left-hand side. The original hcp crystal is shown in the lower part of the figure.

In both Figs. 2 and 3, the nucleation seemed to occur at a definite spot on the cell wall, and the nucleated seed grew into the superfluid phase. Though we could not see that definite spot on the wall, we repeated the experiment many times and confirmed that each event showed the same behavior.

It is shown that the structural transformation proceeds with the nucleation of the new phase in the superfluid and replacement of the original crystal by the new one. The original crystal played no role. This may be because the crystal growth is so rapid even at 1.4 K and it is much easier for the new phase crystal to be nucleated on the wall contacting superfluid and to grow to macroscopic size than to change the structure in the original crystal.

The hcp crystal showed a clear flat plane in the growing process, implying there is a strong anisotropy in the growth coefficient even at this high temperature. The flat plane is most likely [0001]. In the hcp of solid ⁴He, the sound velocity of the longitudinal mode exhibited strong directional dependence from *c* axis.¹⁹ The sound velocity measurement when the space between the two transducers was completely

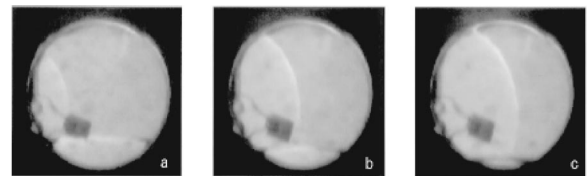


FIG. 3. Crystal shapes at the transition of T_{c1} in the warming process. A new bcc crystal is coming from the left (rounded line). The original hcp crystal lies in the lower part of the cell. The tiny square dark shadow is the heater. The time interval between (a) and (c) is about 500 msec.

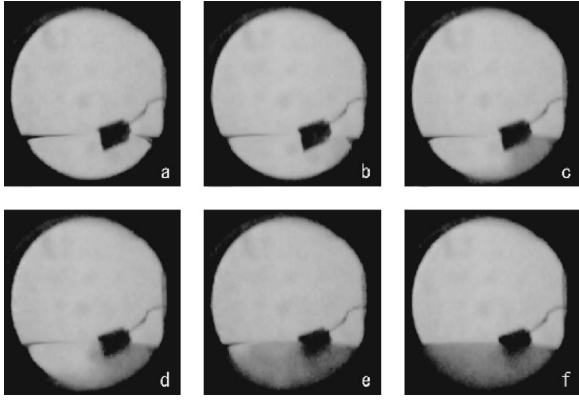


FIG. 4. Crystal shapes at the transition of T_{c2} in the warming process. The upper region is superfluid and the lower part is the bcc crystal. (a) is the picture just before the transition. From (b) to (c) the new phase region (dark area) begins to develop. In (f), the whole crystal becomes dark, which means the transition is completed. In the dark region the crystal is seen to be broken into small grains and has become opaque.

filled with the solid thus gave us information on the crystal orientation. We could deduce that the flat plane in Fig. 2 was the c plane which was 60° from the sound propagation direction. This is consistent with the angle of the flat plane with respect to the horizontal line in that figure. After the bcc crystal disappeared and the hcp crystal completely took over, the facetlike plane disappeared. The flat surface was only observed during the growing process. It should be noticed that the roughening transition temperature of the c plane is 1.25 K,²⁰ and is well below the observation here.

On the other hand, the bcc crystal is always rounded, implying that the growth coefficient is nearly isotropic. Similar phenomena were observed by a different experimental group.⁴

In contrast, the transition at T_{c2} is quite different. The phase transition occurred inside the original solid itself. The (normal) liquid played no important role in the transition. A good transparent crystal was prepared below the lambda point and the temperature was slowly raised through T_{c2} . When the transition was started in the warming process, an opaque region appeared inside the crystal, which looked like smoke. The smokelike region developed throughout the crystal until the entire crystal was opaque (see f in Fig. 4).

The temperature and pressure monitored simultaneously showed clear jumps at the point when an opaque region first became visible (see Fig. 8), indicating that this opaqueness was the transition. “Opaque” as used here means that many hcp grains of different orientation were produced. The grains might have grown slightly in size as the transition proceeded, but no grains appeared to wet each other. The crystal did not become transparent even if annealed for more than an hour.

Next, the temperature was lowered to go back through the transition from hcp to bcc (cooling), and the opaque crystal gradually became transparent. The smokelike region disappeared. It appeared that each grain remembered its original site. Here the wall did not play any role. There must be many dislocations or defects in the crystal; the memory, if it existed, must be kept in these defects and the transition trig-

gered near such defects. There are studies on the nucleation on martensitic transition in metals triggered by the soft mode near the defects.²¹ Unfortunately, we could not control the number of the defects in order to examine their influence on the nucleation. Our attempt to make a good crystal above T_{c2} to test this opaque phenomenon in the cooling process (from hcp to bcc) was not successful.

The dynamic motion of the crystal observed at T_{c1} was not seen here and the overall crystal shape did not change during the transition. The phenomenon is very much reminiscent of martensitic transition.

The term “martensitic transition” is used for a phase change with no mass diffusion and in martensitic transition the nucleated seed often grows as fast as the speed of sound. The speed of the transition at T_{c2} was not greatly different from that at T_{c1} . The present observation can be called a martensiticlike transition in solid ^4He . Here, the crystal was not deformed but was cracked into many grains.

Comparing the results at T_{c1} and T_{c2} , we can state that the superfluid plays a very important role in changing the crystal structure. New ^4He crystal grew in the superfluid first and it took over the original crystal. Without superfluid, the structure of the ^4He crystal changed like an ordinary martensitic transition.

B. Nucleation probability function

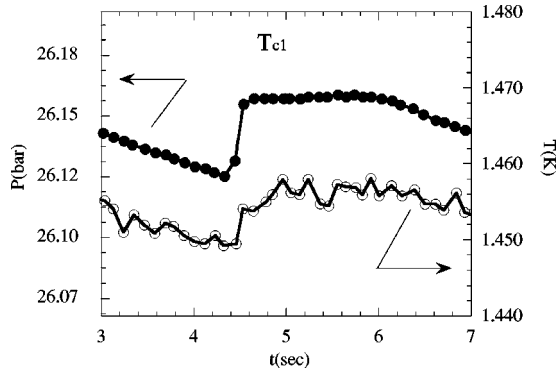
As mentioned in the introduction, if we apply the homogeneous nucleation model to the present bcc-hcp transition of ^4He , it gives an unbelievably small transition probability. According to Hansen,⁵ the ground-state energy difference between hcp and bcc solid is a few tenths of a degree per atom. If we assume the energy difference at the observed average supercooling (superheating) temperature width to be $\delta T \sim 5$ mK/atom, we get $\Delta F/k_B T \sim 10^3$, which results in the incredibly small transition probability of $\sim e^{-1000}$. But the transition definitely occurred with $\delta T \sim 5$ mK of supercooling. It is probable that the transition was triggered by the heterogeneous effects, such as the wall or the defects in the solid. Unfortunately, there is no inhomogeneous nucleation model available with which to analyze the nucleation probability in this study. We therefore used the homogeneous nucleation model just to quantify the event for analysis.

Since the transition obviously occurs stochastically, we repeated the experimental run to pass through the transition point as many times as possible. The transition was monitored by jumps in both temperature and pressure. Figures 5–8 show examples of the temperature and pressure jump at each transition point for both cooling and warming. According to Ref. 2, the transition probability $w(t)$ can be expressed as

$$\frac{dN}{dt} = -\omega(t)N,$$

$$N = N_0 e^{-\omega(t)t}, \quad (2)$$

where $\omega(t)$ is the transition probability at time t , and N is the number of events which have not set in the transition, while N_0 is the total number of trials. So $N_0 - N$ is thus the number

FIG. 5. Temperature and pressure jump at T_{c1} in cooling.

of events which have exhibited the transition. The transition probability ω is given by the Arrhenius formula as

$$\omega = \omega_0 \exp\left(-\frac{\Delta E}{kT}\right), \quad (3)$$

where ω_0 is the trial frequency of the order of $k_B T / \hbar$ and ΔE is the energy barrier which separates the two phases.

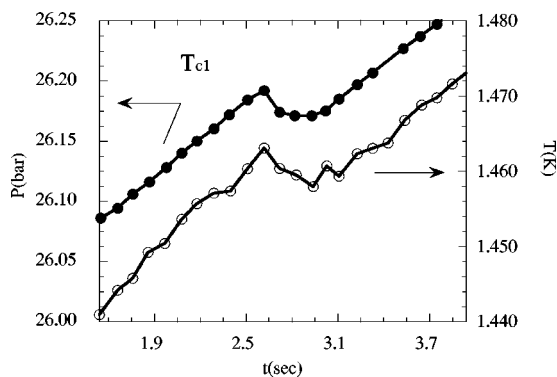
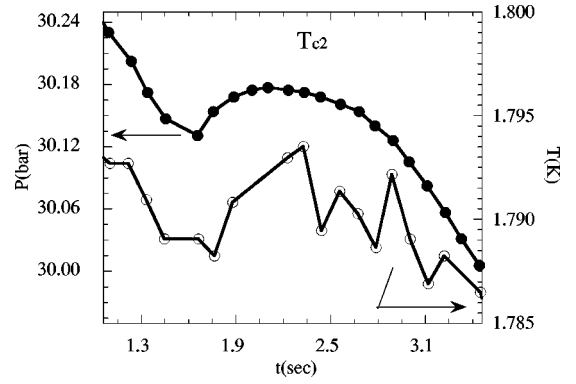
Here we changed the temperature at a constant rate through the transition temperature, as $\delta T = ct$, with c in the range of 0.1–0.5 sec/mK. So the observed nucleation rate, $\Sigma = (N_0 - N)/N_0$, is expressed as

$$\Sigma = (N_0 - N)/N_0 = 1 - \exp\left[-\frac{\delta T}{c} \Gamma_0 \exp\left(-\frac{\Delta E}{kT}\right)\right]. \quad (4)$$

To plot the observed transition rate as a function of δT , we needed to determine the transition temperatures precisely; this was not easy, due to the stochastic character of the transition. We estimated them to be $T_{c1} = 1.457$ K ($P_{c1} = 26.168$ bars) and $T_{c2} = 1.778$ K ($P_{c2} = 30.212$ bars), so that all supercooled and superheated transition events should be plotted consistently in the P - T diagram.

The number of events ($=\Sigma$) is shown in Figs. 9 and 10 as a function of δT , which is the temperature deviation from T_{c1} or T_{c2} . For the cooling case at T_{c2} , the expanded graph is plotted in Fig. 11, since the degree of supercooling is small compared to the degree of superheating.

To fit the data to Eq. (4), the functional form of ΔE has to be known. The problem is that the form of ΔE is not known

FIG. 6. Temperature and pressure jump at T_{c1} in warming.FIG. 7. Temperature and pressure jump at T_{c2} in cooling.

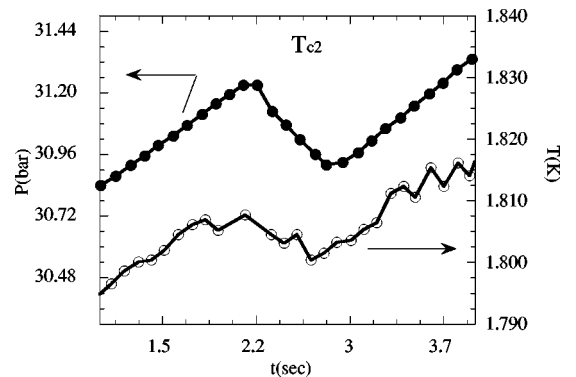
for any case of the present structural transition as a function of temperature deviation δT . But we can assume the general functional form as $\Delta E = A |\delta T - \delta T_{cr}|^{3/2}$. δT_{cr} is the limit of metastability, where the transition occurs without nucleation. This $3/2$ power law is believed to hold in general.²

The solid lines in Figs. 9–11 are the fitted functions of Eq. (4). Here, $\delta T/c$ is replaced with the typical time interval ($=\tau_0$) needed for the transition. The fitting parameters are A and δT_{cr} .

As clearly shown in these figures, the fitting is surprisingly good, and we obtained the following values for the parameters from this fit. To get the measure of the width of supercooling (superheating), we define $\delta T_{1/2}$ as δT which gives $\Sigma = 1/2$. $\delta T_{1/2}$ is easier to use in grasping the width of the transition probability than the parameter A . The results are as follows: At T_{c1} , $[A/k_B T]^{cooling} = 0.0236$, $[A/k_B T]^{warming} = 0.0373$, $[\delta T_{1/2}]^{cooling} = -10.5$ mK, $[\delta T_{1/2}]^{warming} = 4.5$ mK. At T_{c2} , $[A/k_B T]^{cooling} = 0.237$, $[A/k_B T]^{warming} = 0.0136$, $[\delta T_{1/2}]^{cooling} = -2.6$ mK, $[\delta T_{1/2}]^{warming} = 23.5$ mK.

The fitting also produces δT_{cr} 's, but due to the very singular behavior of the function (4), the error of δT_{cr} can be very large, so the estimation of δT_{cr} 's should be done very carefully. We estimated δT_{cr} by several trials of fitting with reasonable results. The following values were obtained; At T_{c1} , $[\delta T_{cr}]^{cooling} = -18 \pm 2$ mK, $[\delta T_{cr}]^{warming} = 8 \pm 1$ mK. At T_{c2} , $[\delta T_{cr}]^{cooling} = -4.5 \pm 1$ mK, $[\delta T_{cr}]^{warming} = 37 \pm 3$ mK.

As expected from the shape of Eq. (4), the transition rate

FIG. 8. Temperature and pressure jump at T_{c2} in warming.

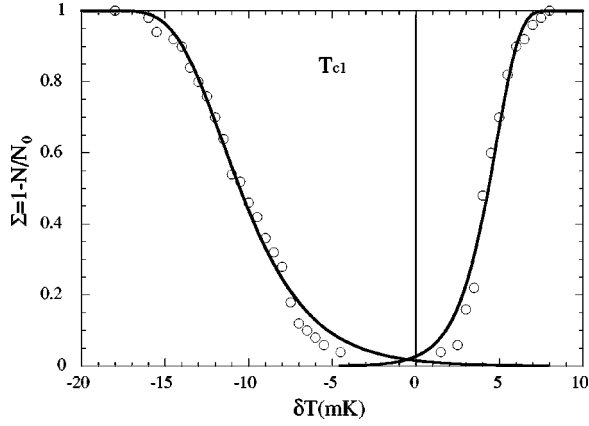


FIG. 9. Transition rate $\Sigma = 1 - N/N_0$ at T_{c1} as a function of δT , the temperature deviation from the transition point. Solid lines are the fitted function. See text for details.

has an asymmetrical shape. The asymmetry means that for small $|\delta T|$ the supercooling (superheating) easily occurs, and as $|\delta T|$ enlarges, the transition rate suddenly gets close to 1. The result obtained here definitely has this tendency and the transition was found to occur stochastically like the model of Eqs. (3) and (4).

Let us first discuss the results at T_{c1} . In this case, the new phase seed is nucleated on the wall in contact with the superfluid, as described in the preceding section. It is seen from the figure that supercooling is more likely than superheating. The median value $\delta T_{1/2}$ is -10.5 mK in the case of supercooling and $+4.5$ mK in the case of superheating. This means that bcc solid is more easily nucleated than hcp solid; this is qualitatively understood from the surface tension difference of hcp and bcc against superfluid.⁴ The surface tension of hcp solid against the liquid is about 25% larger than that of bcc at T_{c1} ,⁷ which is an enormous difference compared to the very small bulk energy difference.

The order of the barrier height ΔE could be estimated from $\delta T_{1/2}$.³ If it is expressed as $\Delta E_{1/2}$, the following values are obtained: At T_{c1} , $\Delta E_{1/2}^{cooling} \sim 42$ K, $\Delta E_{1/2}^{warming} \sim 39$ K. The finding of 42 and 39 K in the cooling and warming

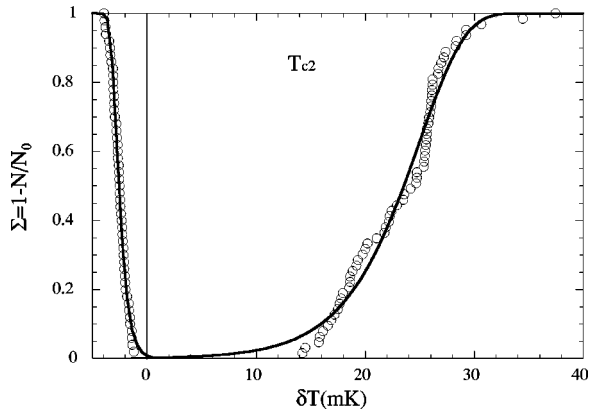


FIG. 10. Transition rate $\Sigma = 1 - N/N_0$ at T_{c2} as a function of δT , the temperature deviation from the transition point. Solid lines are the fitted function. See text for details.

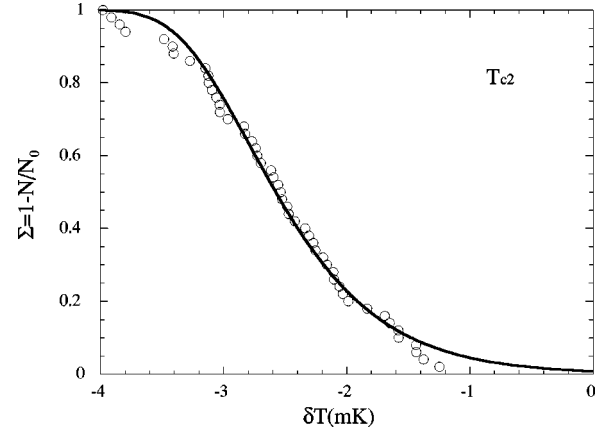


FIG. 11. Transition rate $\Sigma = 1 - N/N_0$ at T_{c1} as a function of δT , the temperature deviation from the transition point. Solid lines are the fitted function. See text for details.

process, respectively, is a consequence of smaller $\delta T_{1/2}$ in warming than in cooling. It is difficult to calculate the energy barrier from the microscopic model to compare with those obtained values.

With regard to the results at T_{c2} , the new phase was nucleated at many sites inside the crystal. In Figs. 10 and 11, the results are also well reproduced by Eq. (4). It is interesting that the model can be applied for the martensiticlike transition observed in solid ^4He . The present martensiticlike transition occurs in various sites in the crystal at almost the same time. It is again surprising that the transition rate is well reproduced by the present model. It may be that the very first nucleation determines the entire transition.

Similarly, $\Delta E_{1/2}$ at T_{c2} is obtained as follows: $\Delta E_{1/2}^{cooling} \sim 50$ K, $\Delta E_{1/2}^{warming} \sim 54$ K. The outstanding feature of Fig. 10 is its large asymmetry between warming and cooling. In the warming process, $\delta T_{1/2}$ is 23.5 mK, whereas it is -2.6 mK in the cooling process. It is curious that $\Delta E_{1/2}$ is not as different as the case of $\delta T_{1/2}$.

It is true that the surface tension of hcp against liquid is also higher than that of bcc at T_{c2} , so the superheating is expected to be larger than the supercooling, but the difference between Figs. 9 and 10 is too big. The supercooling width is too small. If the new solid phases are nucleated without the liquid playing any role, the interfacial tension between hcp and bcc should be the same for cooling and warming, and the asymmetry between cooling and warming should not be as great.

One should pay attention to the fact that T_{c2} ($= 1.778$ K) is very close to the lambda point (1.768 K) on the melting curve. Although most nucleation events occurred above the superfluid transition point, these transition points were in the critical region of the superfluid transition. The heat capacity on the liquid side becomes divergently large, and there may be a big thermal fluctuation which might trigger the transition to bcc. If this were the case, it would mean the liquid contributed to the nucleation in some way. But this is just a speculation at the moment and there is no experimental evidence of this fluctuation.

It is obvious that without any nucleation center the tran-

sition cannot occur. Then, what is the nucleation center in the martensiticlike transition observed in the present study? The dislocations would appear to play an important role but we have no information about those defects at present. An experiment preparing a dislocation should be very interesting but will be very difficult.

Another interesting observation is that the superheated melting curve, that is the melting curve between bcc solid and liquid, is somewhat higher than the equilibrium (hcp solid-liquid) one. For example, at $\delta T = 30$ mK, δP is about 150 mbar; this is rather large. Hopefully, these results provide important information about the equation of the state of solid ^4He at a finite temperature.

IV. CONCLUSION

We have investigated the structural transition of solid ^4He between bcc and hcp on the melting pressure by optical observation. A couple of interesting and important results are recognized.

At the transition of $T_{c1} (= 1.457 \text{ K})$, where solid ^4He coexists with superfluid, the new phase was nucleated at the wall contacting superfluid and grew into the superfluid phase. At the same time, the original crystal gradually melted and was finally replaced completely by the new phase and the transition was completed. The situation is the same for the case of warming and cooling. It is interesting that the original crystal does not appear to play any role.

During the transition, hcp crystal shows a clear facetlike plane, indicating a strong anisotropy in the growth coefficient even at this temperature which is higher than the first roughening transition temperature. When bcc crystal is growing, it is completely rounded, showing that the growth coefficient is isotropic.

At the transition temperature of $T_{c2} (= 1.778 \text{ K})$, on the other hand, where the crystal coexists with normal liquid, the behavior is quite different. The crystal structure is changed in

the original crystal itself, as expected for an ordinary solid. The crystal became opaque when the transition from bcc to hcp occurred. It is believed that the crystal cracked into small grains and the many grains produced scattered the light. This is reminiscent of the martensitic transition, although there is no clear evidence it was the same.

Comparing these observations at T_{c1} and T_{c2} , it is clear that superfluid has a special function in the structural transition. Its detailed mechanism, however, is not understood.

The transition was analyzed to clarify the nucleation nature of the present first-order transition. Fifty to sixty transition events were accumulated and fitted to the standard nucleation model. Though the transition was obviously initiated by “something” heterogeneous, the result was beautifully reproduced by the model, although the reason is not clear.

These analyses did clarify several interesting features, however. There is a big asymmetry in warming and cooling for both transition temperatures. The transition to bcc is always easier than that to hcp. In the transition at T_{c1} , this can be understood qualitatively because of the surface tension difference against superfluid: surface tension of hcp is 25% higher than that of bcc. But in the transition at T_{c2} , the liquid may not be involved, so that there is no explanation why the transition to bcc is easier than to hcp. The width of supercooling at T_{c2} is very small. This is still a mystery.

In conclusion, the present study opened a different aspect of the structural transition of solid ^4He with superfluid and normal liquid. Much more work remains to be done.

ACKNOWLEDGMENTS

The authors would like to thank H. Fujii for his contribution to the early stage of this work and also Dr. Ryuji Nomura for fruitful discussions. This work was partly supported by a grant-in-aid from the Ministry of Education, Science, Sports, Culture and Technology of Japan.

¹S. Balibar and P. Nozières, *Solid State Commun.* **92**, 19 (1994).

²J.P. Ruutu, P.J. Hakonen, J.S. Penttila, A.V. Babkin, J.P. Saramaki, and E.B. Sonin, *Phys. Rev. Lett.* **77**, 2514 (1996).

³S. Balibar, T. Mizusaki, and Y. Sasaki, *J. Low Temp. Phys.* **120**, 293 (2000).

⁴T.A. Johnson and C. Elbaum, *J. Low Temp. Phys.* **107**, 317 (1997).

⁵J.P. Hansen, *Phys. Lett.* **30A**, 214 (1969).

⁶S. Moroni, F. Pedeviva, S. Fantoni, and M. Boninsegni, *Phys. Rev. Lett.* **84**, 2650 (1996).

⁷F. Gallet, P.E. Wolf, and S. Balibar, *Phys. Rev. Lett.* **52**, 2253 (1984).

⁸P.J. Hakonen, M. Krusius, M.M. Salomaa, and J.T. Simola, *Phys. Rev. Lett.* **54**, 245 (1985).

⁹P. Schiffer, D. D. Osheroff, and A. J. Leggett, *Progress in Low Temperature Physics*, edited by W. P. Halperin (Elsevier, New York, 1995), Vol. XIV.

¹⁰W. Schwarz, O. Blaschko, and I. Gorgas, *Phys. Rev. B* **46**, 14 448 (1992).

¹¹H. Abe, K. Ohshima, T. Suzuki, and S. Hoshino, *Phys. Rev. B* **49**, 3739 (1994).

¹²W. Schwarz and O. Blaschko, *Phys. Rev. Lett.* **65**, 3144 (1990).

¹³Y. Okuda, S. Yamazaki, T. Yoshida, Y. Fujii, and K. Matsumoto, *J. Low Temp. Phys.* **113**, 775 (1998).

¹⁴A.J. Dahm, *Cryogenics* **35**, 71 (1995).

¹⁵G.C. Straty and E.D. Adams, *Rev. Sci. Instrum.* **40**, 1393 (1969).

¹⁶E.R. Grilly, *J. Low Temp. Phys.* **11**, 33 (1973).

¹⁷Model 2500, Andeen-Hagerling, Inc., 31200 Bainbridge Road, Cleveland, OH 44139-2231.

¹⁸Model 204, Setra Systems Inc., 159 Swanson Road, Box Borough, MA 01719.

¹⁹D.S. Greywall, *Phys. Rev. A* **3**, 185 (1971).

²⁰P.L. Wolf, F. Gallet, S. Balibar, E. Rolly, and P. Nozières, *J. Phys. (France)* **46**, 1987 (1985).

²¹Y.N. Gornostyrev, M.I. Katsnel'son, A.R. Kuznetov, and A.V. Trefilov, *JETP Lett.* **70**, 380 (1999).